

Article

Coating of Polyetheretherketone Films with Silver Nanoparticles by a Simple Chemical Reduction Method and Their Antibacterial Activity

Andrés Felipe Cruz-Pacheco ¹, Deysi Tatiana Muñoz-Castiblanco ¹,
Jairo Alberto Gómez Cuaspué ¹, Leonel Paredes-Madrid ², Carlos Arturo Parra Vargas ¹,
José Jobanny Martínez Zambrano ¹ and Carlos Andrés Palacio Gómez ^{3,*}

¹ Facultad de Ciencias, Universidad Pedagógica y Tecnológica de Colombia, Tunja 150003, Colombia; andresfelipe.cruz@uptc.edu.co (A.F.C.-P.); deysi.munoz@uptc.edu.co (D.T.M.-C.); jairo.gomez01@uptc.edu.co (J.A.G.C.); carlos.parra@uptc.edu.co (C.A.P.V.); jose.martinez@uptc.edu.co (J.J.M.Z.)

² Faculty of Mechanic, Electronic and Biomedical Engineering, Universidad Antonio Nariño, Tunja 150002, Colombia; paredes.leonel@uan.edu.co

³ Faculty of Sciences, Universidad Antonio Nariño, Tunja 150002, Colombia

* Correspondence: carlospalacio@uan.edu.co; Tel.: +57-(8)-744-7564 or +57-(8)-744-7569 or +57-(8)-744-7566

Received: 10 December 2018; Accepted: 30 January 2019; Published: 2 February 2019



Abstract: The coating of polymeric substrate polyetheretherketone (PEEK) with silver nanoparticles (AgNPs) was carried out by a wet chemical route at room temperature. The coating process was developed from the Tollens reagent and D-glucose as reducing agent. The resulting composite exhibited antimicrobial activity. The PEEK films were coated with a single layer and two layers of silver nanoparticles in various concentrations. The crystallographic properties of the polymer and the silver nanoparticles were analyzed by X-ray diffraction (XRD). Fourier transform infrared spectra (FTIR) show the interaction between the silver nanoparticles with the polymeric substrate. Transmission electron microscope (TEM) images confirmed the obtaining of metallic nanoparticles with average sizes of 25 nm. It was possible to estimate the amount of silver deposited on PEEK with the help of thermogravimetric analysis. The morphology and shape of the AgNPs uniformly deposited on the PEEK films was ascertained by the techniques of scanning electron microscopy (SEM) and atomic force microscopy (AFM), evidencing the increase in the amount of silver by increasing the concentration of the metal precursor. Finally, the antibacterial activity of the films coated with Ag in *Escherichia coli*, *Serratia marcescens* and *Bacillus licheniformis* was evaluated, evidencing that the concentration of silver is crucial in the cellular replication of the bacteria.

Keywords: AgNPs; antibacterial coatings; polyetheretherketone films; tollens method

1. Introduction

Currently, bacterial growth is the main problem of air purification systems such as heaters, air-conditioning and ventilators that are used indoors [1,2]. Some microorganisms are adhered to and absorbed by the parts of the air purifying systems which return to the environment under operational conditions, spreading pathogenic bacteria not only to humans but also to plants and animals [3]. Among the bacteria that are found in the environment and are scattered by air purifying equipment are *Escherichia coli*, *Bacillus subtilis*, *Staphylococcus aureus* and others such as *Serratia marcescens* that cause diseases such as gastroenteritis, urinary tract infections, meningitis and brain abscesses, in addition to pathogenic bacteria that also affect plants and cause cell death such as *Bacillus licheniformis* [4,5]. The alternative to this problem for a long time, has been the combination of air-purifying equipment

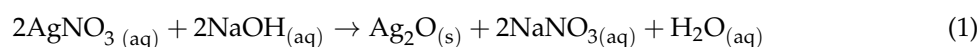
filters with nanocoatings that inhibit bacterial growth, using various polymeric materials such as polyimide, polyurethane, polyacrylonitrile and polysulfone, which has generated contamination and low resistance to exposure of the various environmental effects [6,7]. For this reason, one of the polymers that promises to be efficient as a multifunctional material in the design of filters of air purification equipments is polyetheretherketone (PEEK). This semicrystalline thermoplastic polymer formed by an aromatic chain, combines ketone and ether functional groups between the aryl rings with a mechanical strength stable at high temperatures and resistance to most inorganic and organic substances in comparison with other polymers derived from the polyaryletherketone family (PAEK) [8–10]. These characteristics make PEEK an ideal material for various applications such as components in filters for air decontamination and as complements in decontaminating systems, using effective coatings based on silver nanoparticles with high activity in low concentrations [11–14]. In this sense, several methods have been used to functionalize the PEEK surface, among the most common being the sputtering and plasma deposition techniques [9,15,16]; however, deposition by means chemical routes have attracted great interest due to its simplicity and low cost [17]. Among chemical methods, the deposition of silver nanoparticles using the Tollens reagent has been studied for its simplicity, fast deposition and control of nanoparticle size, the use of non-toxic reagents being one of the most clear benefit of this procedure [18]. This green method allows a silver surface formed by homogeneously distributed nanoparticles in the substrate to be obtained, where the reduction of the ammoniacal silver complex takes place when a monosaccharide as glucose is used as a reducing agent. This results in high antibacterial effectiveness due to the development of small silver (Ag) particle sizes [19,20].

Under the above considerations, the present study aims to obtain polyetheretherketone films coated with various concentrations of silver by a simple chemical reduction method, which contributes to the development of deposition methodologies of silver nanoparticles in polymeric substrates, without the need to use expensive equipment and avoiding the use of polluting reagents. In the same way, the synthesis method using diamoniacal complexes of silver and glucose as a green reducing agent has the advantage of controlling the size and distribution of the AgNPs coated in the PEEK polymer, favoring antibacterial activity against *E. coli*, *S. marcescens* and *Bacillus licheniformis* for potential biomedical applications.

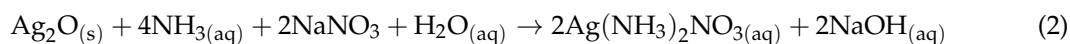
2. Materials and Methods

2.1. Synthesis of Silver Nanoparticles and Coating of Polyetheretherketone (PEEK) Films

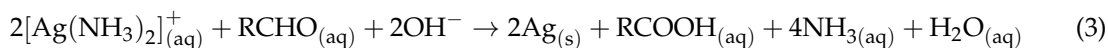
Polyetheretherketone (PEEK) films were coated with 1 and 2 layers of silver nanoparticles (AgNP), reducing ammoniacal silver complexes with glucose in aqueous medium at room temperature. AgNO₃ (99.9%) was purchased from Sigma-Aldrich (Saint Louis, MO, USA), NaOH (99%), Ammonia (25%) and D-Glucose (99%) was obtained from Merck (Darmstadt, Germany). The PEEK film used was Sigma-Aldrich with a thickness of 0.006 mm. The PEEK film was washed with sulfochromic solution (concentrated sulfuric acid with potassium dichromate 90%/10%), for 5 min to remove contaminants in the polymer and to facilitate the coating with silver nanoparticles. For the synthesis of silver nanoparticles, Tollens reagent was used [21,22]. Stoichiometric amounts of silver nitrate in different concentrations were available in a glass reactor previously washed with sulfochromic solution. Subsequently a NaOH dissolution (0.5 mol/L) was added to the above solutions producing silver monoxide, as shown in Equation (1) [23,24].



The precipitated silver monoxide was completely dissolved with ammonia (2 mol/L), producing the Tollens reagent (Equation (2)) [25].



The silver nanoparticles (Ag^0) were obtained by chemical reduction of the silver diamine complex with D-glucose (1 mol/L) as a reducing agent, forming gluconic acid [26]. Equation (3) summarizes the previous reaction. At this stage, the PEEK films were immersed in the solution containing the AgNPs in three different concentrations (0.04, 0.08 and 0.12 mol/L). The immersion was done for 5 min at room temperature and under agitation at 250 rpm; this favored the random sequential adsorption of the silver particles on the polymer surface, thus obtaining the PEEK/Ag0.04, PEEK/Ag0.08 and PEEK/Ag0.12 systems with both single and two layers [27,28]. It must be clarified that the two-layer systems were obtained by repeating the aforementioned procedure for a single-layer film.



The PEEK films coated with one and two-layer silver nanoparticles were dried at 100 °C for 2 h to remove remaining water solvent. In this way, the synthesis route using the Tollens reagent and reducing monosaccharides such as glucose contributes to the progress in the deposition of metal nanostructures in polymeric films by chemical methods.

2.2. Characterization of PEEK Films Coated with AgNPs

X-ray diffraction (XRD) measurements of all the coated films were made on a PANalytical X'Pert PRO MPD diffractometer (Bogotá, Colombia), equipped with an Ultra-Fast X'celerator detector and a Bragg–Brentano configuration, using the Cu $K\alpha$ radiation ($\lambda = 1.5418 \text{ \AA}$) between 20° and 90°. The measurements were developed with an acceleration voltage of 40 kV and a current of 20 mA. The average size of the crystalline domains was determined with the Debye–Scherrer equation using the highest intensity peak in the diffraction pattern of each sample [29]. The infrared (IR) spectra were obtained in the Thermo Scientific Nicolet iS50 spectrometer, by the technique of total attenuated reflection (ATR). The IR spectra were processed with a resolution of 4 cm^{-1} in the average IR (4000–400 cm^{-1}). The samples were placed directly on the cell and pressed to carry out the analysis. The spectra were collected and manipulated with the Omnic^R software (version 6.1).

Transmission electron microscopy (TEM) images were obtained from a Tecnai F20 Super Twin TMP (Medellín, Colombia) of a Field Electron and Ion (FEI) microscope, equipped with a system Ion Milling PIPS II Model 695 GATAN (Medellín, Colombia) and Ultramicrotome EM UC7 LEICA (Medellín, Colombia). The thermal analysis was developed in a Seteram Thermobalance equipment. For the analysis, 5 mg of each sample was weighed and placed in an alumina crucible. The sample was subjected to a heating rate from 25 to 700 °C, under an atmosphere of N_2 with a flow of 20 mL/min.

The morphology of the AgNPs on the PEEK films were analyzed by scanning electron microscopy (SEM) without coating in a JSM-6490 JEOL microscope (Tokyo, Japan), with an acceleration voltage of 15 KV, using secondary electron scattering under high vacuum conditions. Energy-dispersive X-ray spectroscopy (EDS) microanalysis was performed on an Inca Energy 250 EDS System LK-IE250 from Oxford, England, UK, equipped with a silicon detector for light elements and resolution of 138 eV. The surface analysis of PEEK films coated with silver was performed in an atomic force microscope (AFM) Asylum Research, model MFP-3D-BIO. The AFM images were analyzed with the Gwyddion software (version 2.49).

2.3. Antibacterial Activity

The antibacterial activity of the films of PEEK with a coating of AgNPs was studied by the disc diffusion method, for which 100 μL of bacterial suspensions in nutrient broth (this medium contains, in g/L: meat extract, 1.0; yeast extract, 2.0; peptone, 5.0 and sodium chloride, 5.0) of *Escherichia coli*, *Serratia marcescens* and *Bacillus licheniformis* with optical density of 0.01 (OD 600) were spread homogeneously on the nutrient agar plate (meat extract B, 3.0 g/L; peptone, 5.0 g/L and agar, 15.0 g/L) [30]. PEEK discs of 6 mm diameter and 0.006 mm thickness with a coating of AgNPs in different concentrations were used. The samples were placed on the agar plate and were kept in the

incubator at 37 °C for 24 h [16]. Each antibacterial test was evaluated in triplicate. The ImageJ software was employed to measure the diameter of the zone of inhibition of the AgNPs deposited on the PEEK under bacterial activity.

3. Results and Discussion

3.1. X-ray Diffraction (XRD)

Figure 1a shows the X-ray diffraction patterns of the PEEK/Ag0.04, PEEK/Ag0.08 and PEEK/Ag0.12 samples with a coating layer. The semicrystalline structure of the PEEK polymer is revealed with the $2\theta = 16^\circ$, 23° and 30° positions, which are assigned to the (110), (220) and (211) facets, respectively [31–33]. The diffraction peaks found at 38° , 44° and 64° corresponding to the (111), (200) and (220) crystal planes of the face-centered cubic structure of the silver (FCC), which are related with JCPDS (No. 89-3722), confirmed the successful reduction process of the Tollens reagent with D-glucose to obtain the first coating layer of the silver nanoparticles in the polyetheretherketone films [22,34,35]. Figure 1b shows the X-ray diffraction patterns of the samples coated with two layers of silver. The crystallinity of the PEEK film is preserved with the deposition of the second layer of silver on the surface of the polymer since there is no decrease in the intensity of the peaks. Similarly, the intensity of the characteristic metallic silver signals is maintained and increased with the second coating process without detriment to the metallic surface.

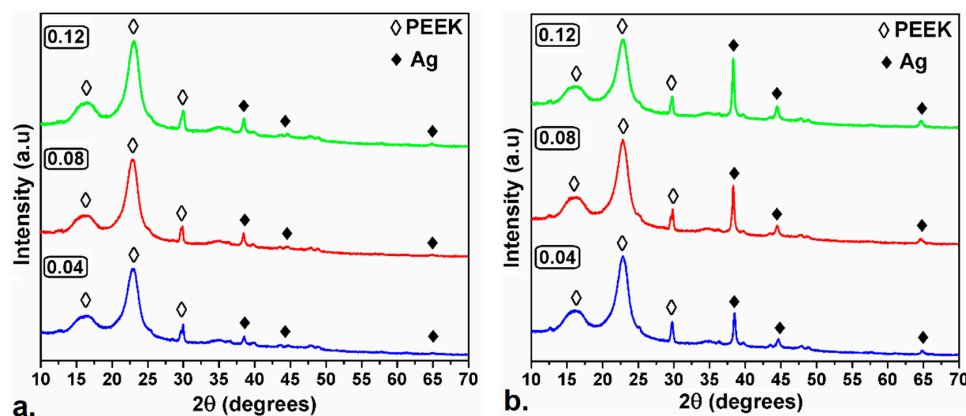


Figure 1. X-ray diffraction (XRD) patterns of polyetheretherketone (PEEK)/Ag0.04, PEEK/Ag0.08 and PEEK/Ag0.12 samples (a) with one coating layer and (b) with two coating layers.

The average sizes of the crystalline domains ($L_{(111)}$) of the silver nanoparticles deposited on the PEEK polymer surface were calculated with the Debye–Scherrer formula. The resulting values are listed in Table 1.

$$L_{(111)} = \frac{k\lambda}{\beta \cos\theta}, \quad (4)$$

where k is the shape factor (0.9), λ is the X-ray wavelength, β is the full width at half maximum (FWHM) in radian, and θ is the Bragg angle in radians corresponding to the most intense (111) diffraction peak [36,37].

Table 1. Data derived from XRD and transmission electron microscopy (TEM) analyses.

Sample	Average Crystal Size by XRD (nm)	FWHM	<i>d</i> -Spacing (nm)	Average Crystal Size by TEM (nm)
PEEK/Ag0.04	23.40	0.3402	0.233	9.1
PEEK/Ag0.08	25.93	0.3066	0.234	9.7
PEEK/Ag0.12	26.48	0.3003	0.234	10.1

FWHM: Full width at half-maximum of the XRD peak.

3.2. Fourier Transform Infrared (FTIR) Spectroscopy

The Figure 2 shows the infrared spectrum of PEEK uncoated and coated with all samples obtained. Figure 2a shows the infrared spectra of PEEK polymer substrates with 1 coating layer. The Fourier transform infrared (FTIR) spectrum of the original PEEK film shows a band at 1647 cm^{-1} of the conjugated ketone stretch (C=O), the bands at 1587 , 1480 and 1410 cm^{-1} corresponding to stretching vibrations of the conjugated carbons on the chains' aromatics. The signal located at 1305 cm^{-1} is characteristic of the flexion between the ketone group and the adjacent carbons. In 1275 cm^{-1} the stretching signal of the ether group is shown. The bands between 1215 and 1100 cm^{-1} are attributed to the deformation flexion in the plane of the C–H bond. The signal at 1008 cm^{-1} can be attributed to the stretched vibrations of the diphenylether bonds of the p-substituents on the aromatic ring (Ar–O–Ar). From 950 to 765 cm^{-1} corresponds to the flexure of deformation outside the plane of the C–H bond [38–40].

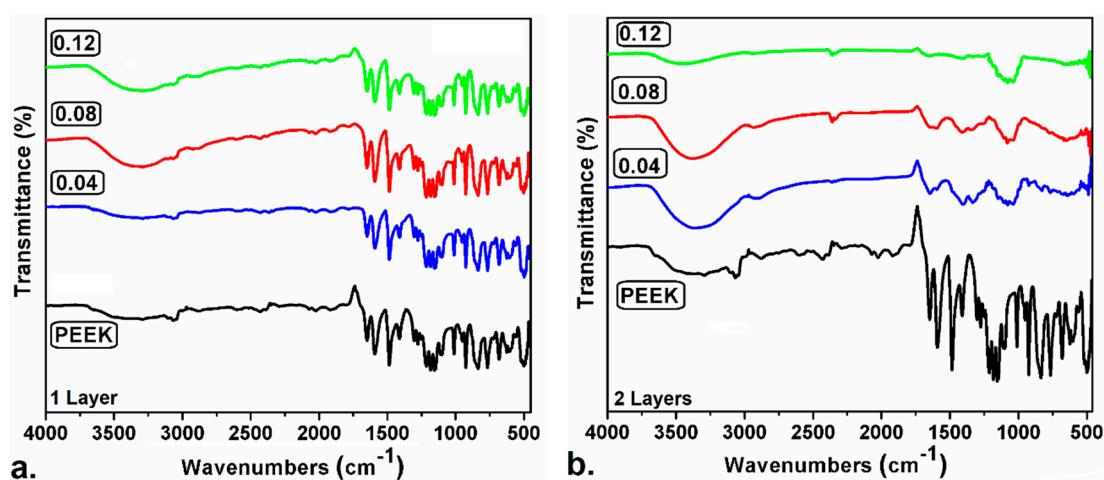


Figure 2. Fourier transform infrared (FTIR) of PEEK/Ag0.04, PEEK/Ag0.08 and PEEK/Ag0.12 samples (a) with one coating layer and (b) with two coating layers.

The main signals of the polyetheretherketone are present in all the samples obtained with a single layer, because the silver deposited in the polymer is small and does not cover the entire film. The signal in 3310 cm^{-1} corresponds to OH groups of NaOH remanent molecules, after the synthesis process of the AgNPs. The OH groups are not water molecules, since the films formed were completely dried. Likewise, in 3060 cm^{-1} the absorption band corresponding to the stretch of the C–H bond of the aromatic ring carbon is evidenced, which loses intensity in the whole spectrum of the coated films, this may be due to the interactions that are generated between the silver nanoparticles and the PEEK [41]. On the other hand, there are no signs of nitro groups (N–O), so it can be said that there are no residual nitrates after the process of synthesis and drying of the formed films.

The FTIR spectra of PEEK films with two layers of coating are shown in Figure 2b. The absorption bands below 3000 cm^{-1} of the PEEK polymer are lost, and new characteristic signals of the silver nanoparticles appear which increase the intensity with the proportion of silver deposited, confirming an optimal distribution of silver on the surface of the polymer. The absorption band at 1070 cm^{-1} is characteristic of the presence of AgNPs [42,43]. The bands at 1650 and 1400 cm^{-1} are of the ketone bond and of the conjugated carbons in the aromatic ring, respectively, which are empty spaces of the polymer where no silver was deposited. In the IR spectrum of the PEEK/Ag0.12 sample with two layers, the characteristic signals of the organic compounds are not present, and this is only the characteristic of the interaction of the silver with the polymer, demonstrating the total coating of the surface area of the polymeric substrate [44].

3.3. Transmission Electron Microscopy (TEM) Analysis

The transmission electron microscopy images of PEEK polymers coated with two layers silver nanoparticles are shown in Figure 3. The analysis of the TEM images showed a distribution of the size of the crystals by means of the ImageJ software; this is shown in Figure 4. The results derived from the statistical analysis corroborated the average sizes of the silver crystals deposited in the polymer and evidenced by the X-ray diffraction patterns using the Debye–Scherrer equation.

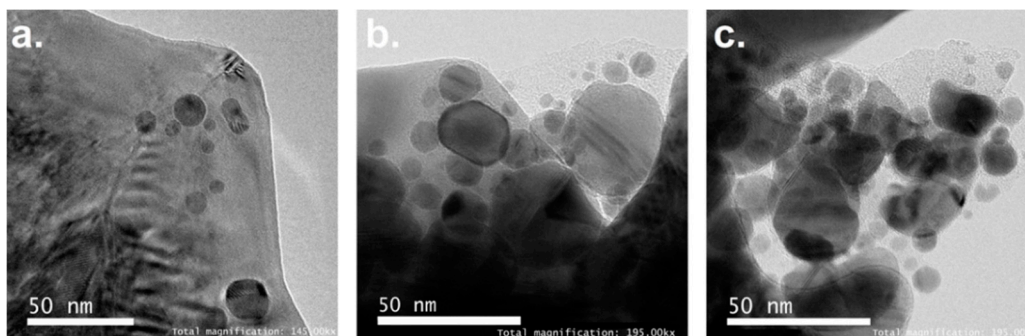


Figure 3. TEM images of (a) PEEK/Ag0.04, (b) PEEK/Ag0.08 and (c) PEEK/Ag0.12. The samples were coated with two layers of AgNPs.

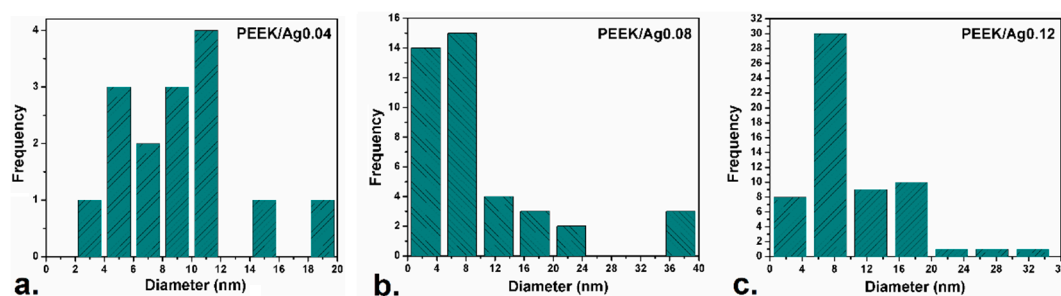


Figure 4. Distribution of the particle sizes determined from the TEM data at 50 nm of the obtained samples with 2 layers. (a) PEEK/Ag0.04, (b) PEEK/Ag0.08 and (c) PEEK/Ag0.12.

The comparison among particle sizes obtained by XRD and TEM are presented in Table 1. The experimental results shown that the silver nanoparticles with the polymer were coated on average by less than 30 nm. Based on previous studies [45], particle dimensions play an important role in the antibacterial activity of the coating and, therefore, this must be monitored in the final coating assembly. In the same way, the synthesis of silver nanoparticles using the Tollens reagent and an economic reducing agent, such as D-glucose, allowed control of the size and shape of the nanoparticles deposited in the PEEK [46]. In the same way, when different concentrations of AgNO₃ are used, the increase in the size of the synthesized nanoparticles is related to the amount of ammonia. By increasing the concentration of silver in the different samples, the amount of ammonia required for the reaction is also increased, thus favoring the stabilization of the complex [Ag(NH₃)⁺]. This phenomenon decreases the amount of Ag⁺ species, which causes the decrease of stable silver nuclei in the reduction process with glucose, and induces the formation of large particles in the growth stage [47–49].

Figure 5 shows the transmission electron microscopy images of the PEEK/Ag0.12 sample cut with ultramicrotome at different magnifications. In Figure 5a,b the obtaining of uniformly sized silver nanoparticles adhered to the PEEK polymer is corroborated by electrostatic forces generated by the high charge of the reduced silver in the synthesis process [17,50]. Likewise, the AgNPs form agglomerates of regular size, which extend throughout the PEEK substrate surface. Figure 5c shows the resistance to friction applied by the diamond tip in the cut with ultramicrotome on the polymer coated with silver nanoparticles. The cut is made in a transversal way allowing the PEEK film (thickness 6 μm) and the metallic silver adhered to the polymer by electrostatic interactions [51] to be observed.

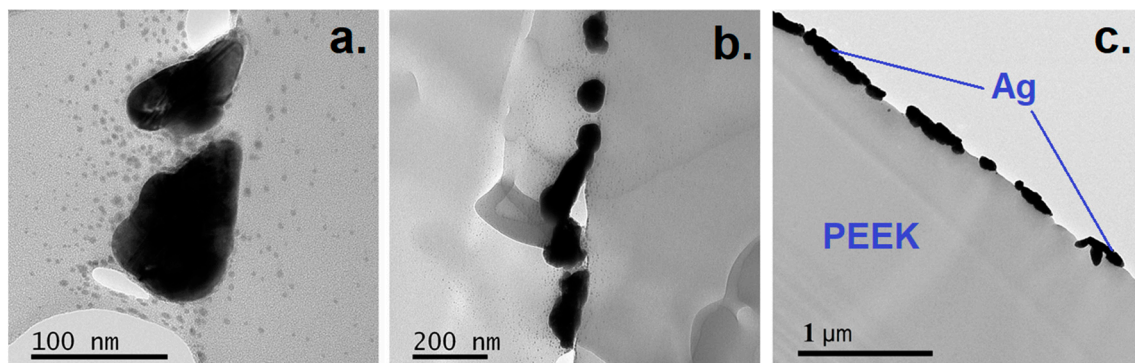


Figure 5. TEM images of the sample PEEK/Ag0.12 with two layers. (a) 100 nm; (b) 200 nm; (c) 1 μ m.

3.4. Thermogravimetric Analysis (TGA)

Thermogravimetric analysis (TGA) of all samples is shown in Figure 6, in which it is clear that PEEK as a thermoplastic polymer exhibits a thermal decomposition above 500 °C. The amount of silver deposited is determined from the difference of pure PEEK and modified PEEK thermograms [52,53]. The temperature at which the difference was taken was 675 °C, since at this temperature the polymer is decomposed as shown in Figure 6 and as reported in the literature [54]. In this sense, for the polymers coated with a single layer of silver nanoparticles in concentrations of 0.04, 0.08 and 0.12 mol/L the amount of silver was 5.9%, 8.12% and 10.8% silver, respectively.

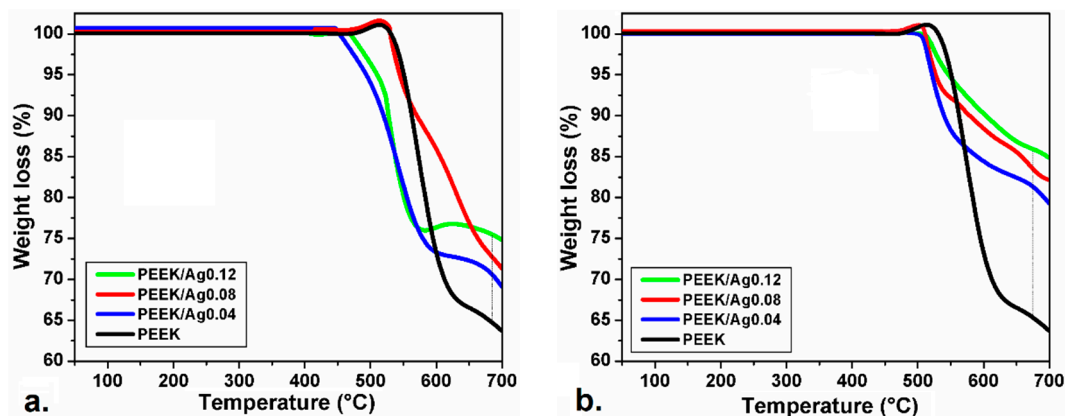


Figure 6. Thermogravimetric analysis (TGA) of uncoated PEEK, PEEK/Ag0.04, PEEK/Ag0.08 and PEEK/Ag0.12 samples (a) with one coating layer and (b) with two coating layers.

The percentages of silver deposited in the polymers coated with two layers of silver nanoparticles were 16.1, 18.5 and 20.99% Ag for the concentrations of 0.04, 0.08 and 0.12 mol/L, respectively. Due to the aromatic structure of the PEEK, a higher amount of residues are obtained (more than 60%) after heating at to 700 °C [31]. This analysis contrasts with the results of X-ray diffraction and FTIR in terms of the proportional amount of silver deposited in the PEEK, but confirm the thermal stability of materials above 450 °C.

3.5. Morphological Evolution and Particle Distribution by Scanning Electron Microscopy (SEM)

The deposition and dispersion of AgNPs in the PEEK was evaluated by scanning electron microscopy at different resolutions. Figure 7 shows the SEM images of different PEEK films with a silver layer on the surface, in which a proportional increase in the amount of silver deposited in the polymer is evidenced by the concentration of AgNO₃ used. Considering that the silver nanoparticles are conductive, the SEM measurements were performed without sample preparation, i.e., no gold or graphite coating was applied before sample measuring. Consequently, the black areas correspond to

the polymer which is not conductive, whereas the white and gray points correspond to silver particles. The homogeneity and distribution of the AgNPs deposited on the polymer surface are quite similar to other synthesis methods; this was possible because experimental conditions allowed controlling the amount of deposited particles, and thus, the formation of agglomerates that increase the density of the solids. The SEM images are congruent with the TEM images shown in Figure 5, in which it is shown that the particles with size greater than 80 nm are composed of aggregates of smaller silver nanoparticles.

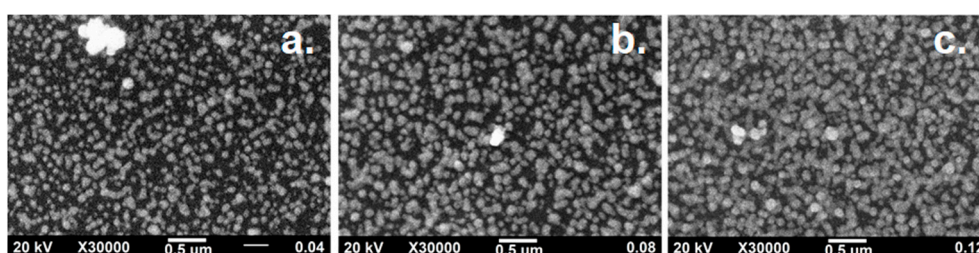


Figure 7. Scanning electron microscopy (SEM) images of the polyetheretherketone coated with one layer of silver nanoparticles in concentrations of (a) 0.04 mol/L, (b) 0.08 mol/L and (c) 0.12 mol/L.

Figure 8 shows SEM images of the PEEK/Ag0.04, PEEK/Ag0.08 and PEEK/Ag0.12 systems with two silver layers. The evolution of the PEEK coating is identified by increasing in the concentration of silver nanoparticles. The empty black areas shown in Figure 7 correspond to PEEK; these are homogeneously filled by silver particles, which cover most of the polymer surface as shown in Figure 8 (when two layers were applied). In the PEEK/Ag0.08 and PEEK/Ag0.12 systems, the appearance of small agglomerations is favored, which were formed by the greater amount of silver ions available in the reaction medium. In this sense, SEM micrographs correlate with the results of XRD, FTIR and TGA, in terms of increasing the proportion of silver on the surface of the polymer, showing the efficiency of the simple chemical reduction method in the deposition of metallic nanoparticles.

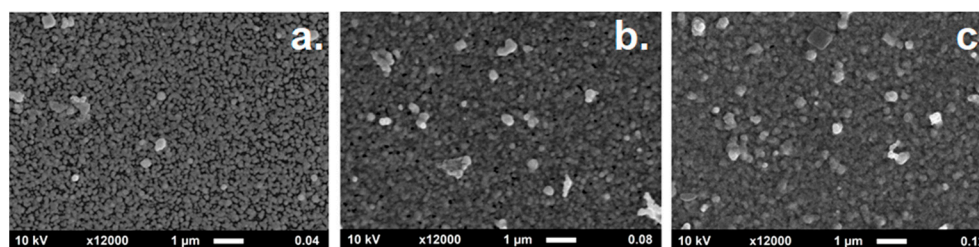


Figure 8. SEM images of the polyetheretherketone coated with two layers of silver nanoparticles in concentrations of (a) 0.04 mol/L, (b) 0.08 mol/L and (c) 0.12 mol/L.

3.6. Energy-Dispersive X-Ray Spectroscopy (EDS) Microanalysis

EDS microanalysis shown in Figure 9, was performed to determine the elemental composition of the PEEK/Ag0.08 system with a single and two layers of AgNPs. The analysis was performed on an area of 600 μm and 500 μm . The analysis was performed on the PEEK/Ag0.08 sample since it was the one that presented the most intense OH absorption band. According to this analysis, it is clear that the present synthesis method provides a high level of purity of the silver nanoparticles deposited in the PEEK polymer, since a residue such as NaOH is in a proportion less than 1%. In the same way, the elemental analysis does not evidence the presence of nitrogen atoms associated with remaining nitrate ions.

The weight percentage of silver shown by the EDS spectra is proportional to the result of TGA, since it is evident that the amount of silver increases with the second layer of silver nanoparticles deposited in the polymer. The difference between TGA and EDS analysis is that in the EDS, only a small

and surface portion of the sample is analysed, while in the TGA a more quantitative portion is taken, being a more relevant result.

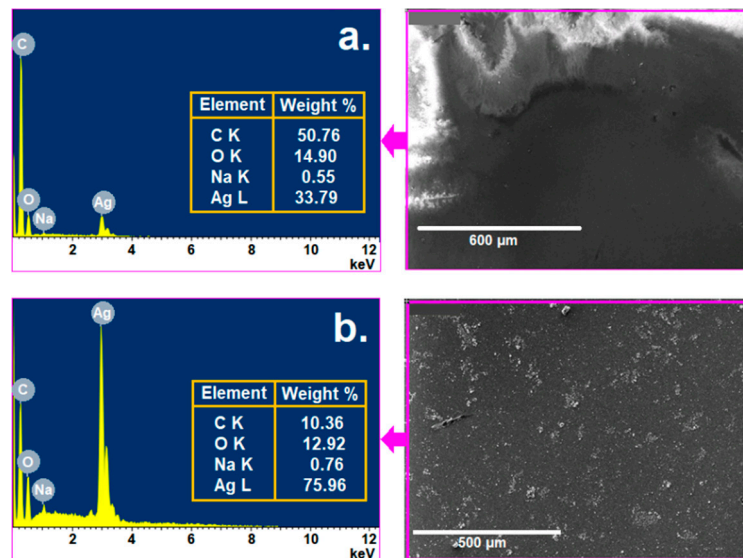


Figure 9. Energy-dispersive X-ray spectroscopy (EDS) microanalysis of the sample PEEK/Ag0.08 with a single (a) and with two layers (b).

3.7. Atomic Force Microscopy (AFM) analysis

Surface analyses of the coated Polyetheretherketone films were evaluated by AFM. Figure 10 shows AFM images of the systems with the first coating layer. The images confirm the homogeneity of the nanoparticles deposited in the PEEK substrate, just as the SEM imaging previously revealed. Likewise, the height of the images is consistent with the TEM analysis, where a coating of the nanometric order with excellent particle distribution on the surface of the polymer was obtained. Figure 10b shows a collapse caused by the piezoelectric tip of the equipment, because the PEEK film and the silver coating are very thin.

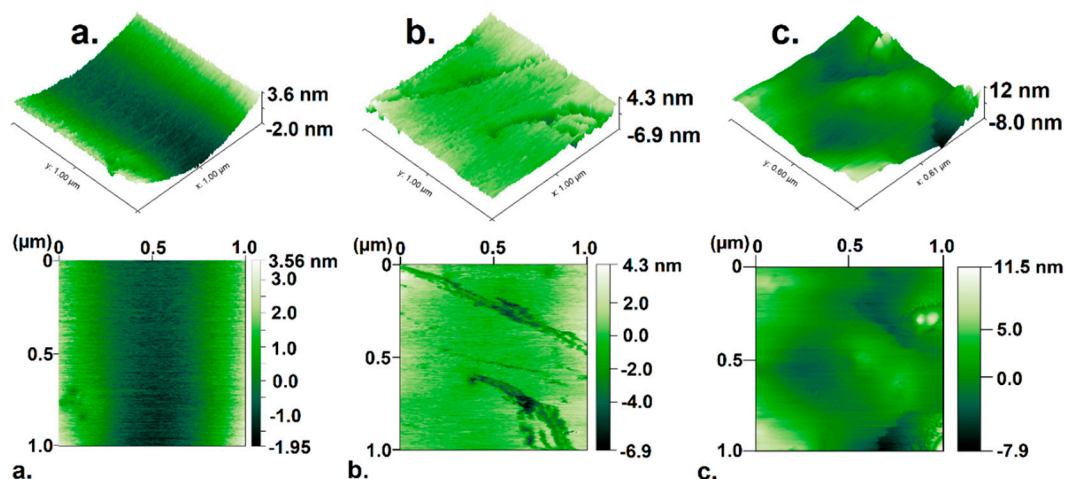


Figure 10. Atomic force microscopy (AFM) images of the (a) PEEK/Ag0.04, (b) PEEK/Ag0.08 and (c) PEEK/Ag0.12 systems with one layer.

The AFM images of the PEEK/Ag systems obtained with two layers of silver are shown in Figure 11. The images represent the remarkable increase in the thickness of each sample obtained with two layers of silver. The PEEK films with two layers of silver deposited on their surface at

concentrations of 0.04 and 0.08 mol/L shown in Figure 11a,b exhibit a small amount of aggregate particles. Figure 11c shows the excellent homogenization in the second stage of coating of the polymer, generating small agglomerations because of the high concentration of silver.

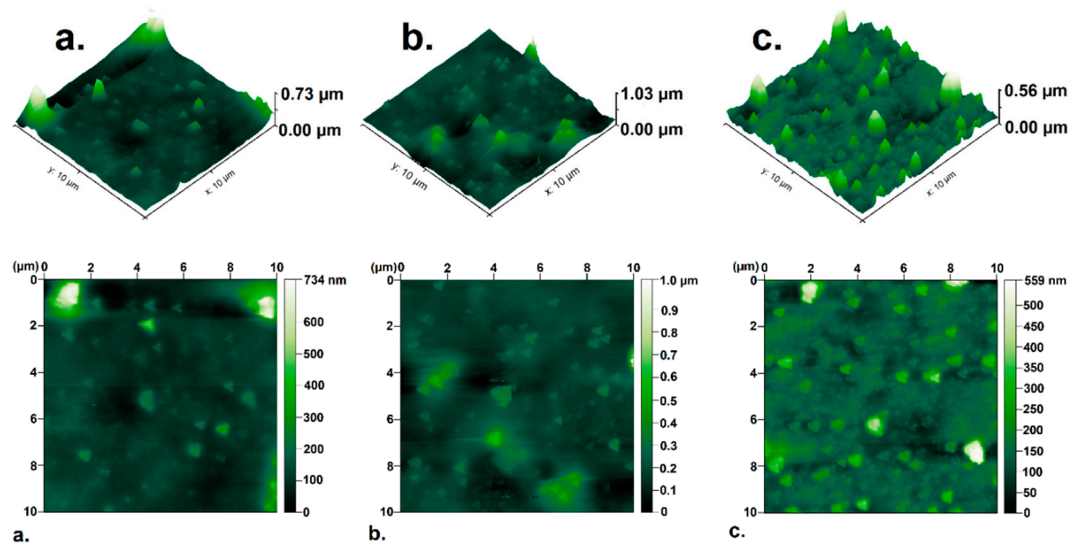


Figure 11. AFM images of the (a) PEEK/Ag0.04, (b) PEEK/Ag0.08 and (c) PEEK/Ag0.12 systems with two layers.

The average thickness of the three samples after the second coating process is in the range between 200 and 300 nm, and increased proportionally with the increase in Ag concentration. In general, the AFM analyses confirm the results by SEM regarding the homogeneous distribution of the silver nanoparticles deposited in the PEEK substrate.

The analysis of the roughness of PEEK materials coated with silver was evaluated with the root mean square (RMS) parameter shown in Table 2. The RMS value is related to the amount of silver deposited in the polymer. When increasing the amount of silver, the average roughness of the material increases forming several nanometric-sized valleys. The PEEK samples coated with a single layer of silver have small surface roughness values, due to the thin layer of silver deposited in the chemical synthesis method. In the same way, samples coated with two layers of silver have higher RMS values according to the quantity of silver nanoparticles deposited on the surface of the polymer [55]. The amount of nanoparticles deposited on both sides of the polymer has an inference in the antibacterial properties. This occurs because more Ag^+ species are generated which are responsible for inhibiting bacterial growth as explained in the following section and as reported by Liu et al. [55]. The surface roughness value also provides information on the adhesion of the silver nanoparticles on the polymer, corroborating the TEM analysis, since as a nanometric-sized coating, electrostatic interactions between the metallic silver and the polymer result [56]. In addition, the surface contact of the nanometer probe with the silver deposited in a single layer does not drag but leaves a groove upon movement, showing the effective adhesion with the polymer as indicated by Wenfei Li et al. [57]. On the other hand, in the samples with two layers the adhesion improves since the entire surface of the polymer is coated with AgNPs increasing the electrostatic interactions.

Table 2. Surface roughness values of the different PEEK samples coated with silver.

Sample	Surface Roughness (nm) Root Mean Square (RMS)
PEEK/Ag0.04 – 1 Layer	0.96 ± 0.3
PEEK/Ag0.08 – 1 Layer	1.54 ± 0.2
PEEK/Ag0.12 – 1 Layer	2.36 ± 0.7
PEEK/Ag0.04 – 2 Layer	56.38 ± 3.7
PEEK/Ag0.08 – 2 Layer	67.44 ± 3.0
PEEK/Ag0.12 – 2 Layer	92.63 ± 1.8

3.8. Antibacterial Test

The antibacterial activity of the PEEK films coated with various concentrations of silver nanoparticles by a green method using the Tollens reagent and a monosaccharide were tested against two Gram-negative bacteria: *Escherichia coli* and *Serratia marcescens* and one Gram-positive bacterium: *Bacillus licheniformis*, evaluating the zone of inhibition by a contact method direct with medium agar as shown in Figures 12–14. The results of the zone of inhibition measured with the ImageJ software are shown in Table 3.

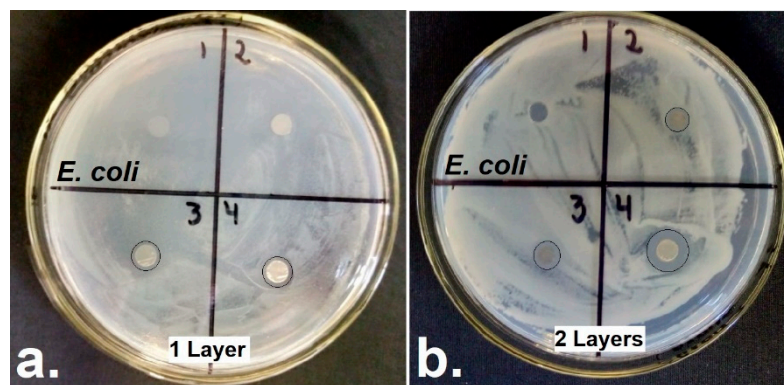


Figure 12. Inhibition zone of the PEEK (1), PEEK/Ag0.04 (2), PEEK/Ag0.08 (3) and PEEK/Ag0.12 (4) coated with one layer (a) and two layers (b) of silver with *Escherichia coli*.

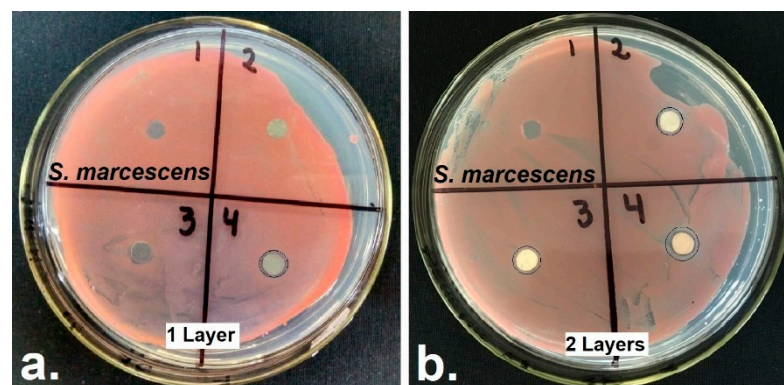


Figure 13. Inhibition zone of the PEEK (1), PEEK/Ag0.04 (2), PEEK/Ag0.08 (3) and PEEK/Ag0.12 (4) coated with one layer (a) and two layers (b) of silver with *Serratia marcescens*.

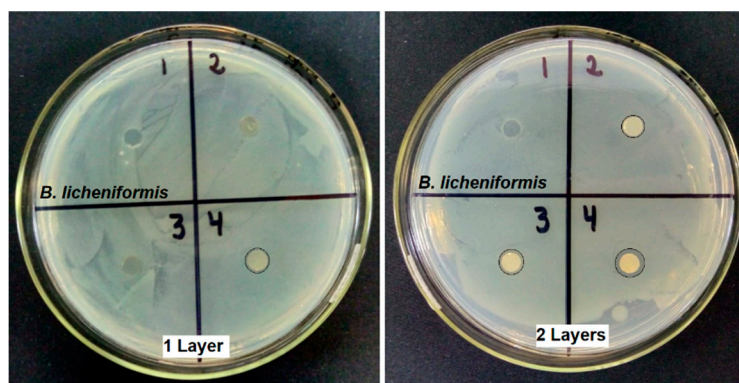


Figure 14. Inhibition zone of the PEEK (1), PEEK/Ag0.04 (2), PEEK/Ag0.08 (3) and PEEK/Ag0.12 (4) coated with one layer (a) and two layers (b) of silver with *Bacillus licheniformis*.

Table 3. Antibacterial activity of silver nanoparticles deposited in PEEK films.

Sample	Diameter of Inhibition Zone (mm) \pm SD		
	<i>E. coli</i>	<i>S. marcescens</i>	<i>B. licheniformis</i>
PEEK	0	0	0
PEEK/Ag0.04 – 1 Layer	0	0	0
PEEK/Ag0.08 – 1 Layer	1.1 \pm 0.2	0	0
PEEK/Ag0.12 – 1 Layer	1.2 \pm 0.2	0.6 \pm 0.2	0.5 \pm 0.1
PEEK/Ag0.04 – 2 Layer	1.2 \pm 0.2	0.8 \pm 0.2	0.5 \pm 0.1
PEEK/Ag0.08 – 2 Layer	1.4 \pm 0.1	0.9 \pm 0.2	0.7 \pm 0.1
PEEK/Ag0.12 – 2 Layer	2.7 \pm 0.3	1.2 \pm 0.3	1.0 \pm 0.2

SD: standard deviation.

For the antimicrobial test, an uncoated PEEK film was used as a control in the six plates, which did not present antimicrobial activity. The amount of silver deposited on the PEEK/Ag0.04 sample with a single layer was not enough to prevent the proliferation of the Gram-negative bacteria shown in Figures 12 and 13, stimulating bacterial growth in the silver-free sites that are shown in the SEM images, similar to that reported by Seuss et al. [30]. While the polymer coated with a layer AgNPs in a concentration of 0.08 mol/L presented inhibition against *E. coli* but not against *S. marcescens*. The PEEK/Ag0.12 system with a single layer and all the samples coated with two layers of AgNPs had antibacterial properties, which increased the zone of inhibition with the amount of Ag⁺ ions deposited in the substrate, favoring the bactericidal effect.

The antibacterial efficiency of PEEK films coated with AgNPs shown in Table 3 was higher for *E. coli* compared to *S. marcescens*, and this was due to the presence of an envelope of two membranes which have different proteins and phospholipids that prevent the passage of silver nanoparticles inside the cells. [16,30,58]. Although the *S. marcescens* bacterium is resistant to traditional antibiotics, the AgNPs synthesized by a green method and deposited on a polymeric PEEK substrate had antibacterial efficiency against this microorganism, because the nanoparticles easily crossed the cytoplasmic membrane due to its small size, causing damage to the organelles of the cell and leading to the death of the microorganism, similar to that described by Baghayeri et al. [59] and Mathew et al. [4].

Figure 14 shows that the uncoated Polyetheretherketone films had no antimicrobial effect on the Gram-positive bacterium *Bacillus licheniformis* similar to a Gram-negative bacterium. Figure 14a,b show that the polyetheretherketone films coated with a single layer of silver nanoparticles in concentrations of 0.04 and 0.08 mol/L did not exhibit antibacterial activity in *B. licheniformis*, while the PEEK/Ag0.12 system and all polymeric films coated with two layers of metallic silver counteracted the growth of Gram-negative bacteria, by releasing silver ions in humid conditions. In addition, the amount of nanoparticles in the culture medium increased the zone of inhibition of bacterium *B. licheniformis* as shown in Table 3 [60,61]. The growth of the Gram-positive bacterium was higher in comparison with

the Gram-negative bacteria, because the bacterium *Bacillus licheniformis* has a thicker peptidoglycan layer in its membrane, which regulates and prevents the path of AgNPs in low concentrations to the cell as indicated by Mathew T. et al. [4]. Similar results with a difference in antibacterial activity were observed by Sikder et al. [62,63] when exploring antibacterial surfaces on PEEK and Ti6Al4V, and such studies were performed in the case of Gram-negative (*E. coli*) and gram-positive (*S. aureus*) bacteria. Apart from the difference in the diameter of inhibition zone, their research also presented SEM images which prove the variance in interactions of Ag⁺ ions with negative and positive strains of bacteria. And therefore, these results show a similar trend to the present work. Likewise, Mosselhy D.A. et al. and Ur Rehman et al. [16,64] described a similar effect to the one reported in this study, where the antibacterial properties increased with the increase of the silver nanoparticle ratio and the humid environment in which the samples were installed, such studies demonstrated the effectiveness of the AgNPs coatings in solid state as an antibacterial system.

The antibacterial mechanism of the silver nanoparticle coatings is possible because of the Ag⁺ ions generated by the conversion of metallic silver into the physiological environment where the antimicrobial evaluation occurs [16]. The silver nanoparticles in cationic form penetrate the cell, deforming the cell membrane, and interacting with some proteins; the silver nanoparticles also interact with the sulfur and phosphorus bases contained in the DNA, causing an interruption in DNA replication and subsequent cell death [36,37]. Likewise, Ag⁺ ions form free radicals that attack respiratory enzymes which are essential for cell replication [45,59].

The zone of inhibition of the three bacteria analyzed was similar in the PEEK/Ag0.12 samples with a single layer and PEEK/Ag0.04 with two layers. This was possible from the homogeneously distributed silver nanoparticles deposited once on the PEEK substrate when AgNO₃ was used in a concentration of 0.12 mol/L. Such particles had a high surface area with particle sizes below 25 nm according to the SEM and AFM analyzes. Finally, the sample with the maximum zone of inhibition against the growth of *E. coli*, *S. marcescens* and *B. licheniformis* was PEEK/Ag0.12 with two coating layers of AgNPs, corroborating the efficacy of the synthesis method by chemical reduction of ammoniacal silver complexes with glucose in obtaining coatings of metallic silver nanoparticles with high surface area [65]. In addition, the increase in the proportion of nanoparticles in the polymeric substrate favors the antibacterial effectiveness by the high liberation of silver ions in the wet conditions of the culture medium as reported by Logeswari et al and Gao et al. [66,67].

4. Conclusions

A method of coating by a chemical route with ammoniacal silver complexes was used to impregnate polyetheretherketone films with silver nanoparticles to inhibit bacterial growth. The characteristic diffraction peaks of PEEK were kept constant by completely coating the surface of the polymer. The intensity of the silver signals in the diffractograms increased with the amount of silver nanoparticles deposited. The average size of the crystalline domains of AgNPs synthesized by a simple chemical reduction method was less than 30 nm using the Debye–Scherrer formula, corroborating the results by statistical analysis with transmission electron microscopy images. The electrostatic interactions between the polymer and the deposited AgNPs were evidenced by FTIR and TEM. The thermograms showed the proportion of silver adhered to the polymeric substrate. The proportional deposition of silver on the surface of the PEEK was evaluated by scanning electron microscopy and atomic force microscopy, revealing the excellent distribution of the particles when they are synthesized with glucose. In addition, it is evident that the second deposition process leaves the polymer with a thickness around 300 nm for all samples. The action mechanism of AgNPs against the bacterial growth of pathogenic microorganisms is influenced by the conversion of metallic silver to Ag⁺. The sample that shows the best antibacterial activity in Gram-positive and Gram-negative bacteria for a possible application in the design of air purification equipment is PEEK/Ag0.12 with two layers, since the excellent distribution of the coating improves contact with bacteria, inhibits the replication process, and favors cell death

Author Contributions: Conceptualization, A.F.C.-P., J.A.G.C. and J.J.M.Z.; Data Curation, A.F.C.-P., D.T.M.-C., J.A.G.C. and J.J.M.Z.; Formal Analysis, A.F.C.-P., D.T.M.-C. and J.A.G.C.; Funding Acquisition, L.P.-M., C.A.P.V., J.J.M.Z. and C.A.P.G.; Investigation, A.F.C.-P., D.T.M.-C., J.A.G.C. and L.P.-M.; Methodology, J.A.G.C.; Project Administration, C.A.P.G.; Resources, C.A.P.V., J.J.M.Z. and C.A.P.G.; Supervision, J.A.G.C., L.P.-M., C.A.P.V., J.J.M.Z. and C.A.P.G.; Validation, L.P.-M. and C.A.P.G.; Writing—Original Draft, A.F.C.-P.; Writing—Review & Editing, A.F.C.-P., J.A.G.C., L.P.-M. and C.A.P.G.

Funding: This work was supported by Universidad Antonio Nariño under the project number 2016216-PI/UAN-2018-635GFM and by Vicerrectoría de Investigación y Extensión de la Universidad Pedagógica y Tecnológica de Colombia.

Conflicts of Interest: The authors declare no conflict of interest.

References

1. Kakinuma, H.; Ishii, K.; Ishihama, H.; Honda, M.; Toyama, Y.; Matsumoto, M.; Aizawa, M. Antibacterial polyetheretherketone implants immobilized with silver ions based on chelate-bonding ability of inositol phosphate: Processing, material characterization, cytotoxicity, and antibacterial properties. *J. Biomed. Mater. Res. Part A* **2015**, *103*, 57–64. [[CrossRef](#)] [[PubMed](#)]
2. Gutarowska, B.; Stawski, D.; Skóra, J.; Herczyńska, L.; Pielech-Przybylska, K.; Połowiński, S.; Krucińska, I. PLA nonwovens modified with poly(dimethylaminoethyl methacrylate) as antimicrobial filter materials for workplaces. *Text. Res. J.* **2015**, *85*, 1083–1094. [[CrossRef](#)]
3. Ki, Y.Y.; Jeong, H.B.; Chul, W.P.; Hwang, J. Antimicrobial effect of silver particles on bacterial contamination of activated carbon fibers. *Environ. Sci. Technol.* **2008**, *42*, 1251–1255. [[CrossRef](#)]
4. Mathew, T.V.; Kuriakose, S. Studies on the antimicrobial properties of colloidal silver nanoparticles stabilized by bovine serum albumin. *Colloids Surf. B Biointerfaces* **2013**, *101*, 14–18. [[CrossRef](#)] [[PubMed](#)]
5. Burman, S.; Bhattacharya, K.; Mukherjee, D.; Chandra, G. Antibacterial efficacy of leaf extracts of *Combretum album* Pers. against some pathogenic bacteria. *BMC Complement. Altern. Med.* **2018**, *18*, 213. [[CrossRef](#)] [[PubMed](#)]
6. Zhu, M.; Xiong, R.; Huang, C. Bio-based and photocrosslinked electrospun antibacterial nanofibrous membranes for air filtration. *Carbohydr. Polym.* **2019**, *205*, 55–62. [[CrossRef](#)] [[PubMed](#)]
7. Le, T.S.; Dao, T.H.; Nguyen, D.C.; Nguyen, H.C.; Balikhin, I.L. Air purification equipment combining a filter coated by silver nanoparticles with a nano-TiO₂ photocatalyst for use in hospitals. *Adv. Nat. Sci. Nanosci. Nanotechnol.* **2015**, *6*, 015016. [[CrossRef](#)]
8. Montero, J.F.D.; Barbosa, L.C.A.; Pereira, U.A.; Barra, G.M.; Fredel, M.C.; Benfatti, C.A.M.; Magini, R.S.; Pimenta, A.L.; Souza, J.C.M. Chemical, microscopic, and microbiological analysis of a functionalized poly-ether-ether-ketone-embedding antibiofilm compounds. *J. Biomed. Mater. Res. Part A* **2016**, *104*, 3015–3020. [[CrossRef](#)] [[PubMed](#)]
9. Wiacek, A.E.; Terpilowski, K.; Jurak, M.; Worzakowska, M. Effect of low-temperature plasma on chitosan-coated PEEK polymer characteristics. *Eur. Polym. J.* **2016**, *78*, 1–13. [[CrossRef](#)]
10. Wu, J.; Li, L.; Fu, C.; Yang, F.; Jiao, Z.; Shi, X.; Ito, Y.; Wang, Z.; Liu, Q.; Zhang, P. Micro-porous polyetheretherketone implants decorated with BMP-2 via phosphorylated gelatin coating for enhancing cell adhesion and osteogenic differentiation. *Colloids Surf. B Biointerfaces* **2018**, *169*, 233–241. [[CrossRef](#)]
11. Joe, Y.H.; Ju, W.; Park, J.H.; Yoon, Y.H.; Hwang, J. Correlation between the antibacterial ability of silver nanoparticle coated air filters and the dust loading. *Aerosol Air Qual. Res.* **2013**, *13*, 1009–1018. [[CrossRef](#)]
12. Bodden, L.; Lümekemann, N.; Köhler, V.; Eichberger, M.; Stawarczyk, B. Impact of the heating/quenching process on the mechanical, optical and thermodynamic properties of polyetheretherketone (PEEK) films. *Dent. Mater.* **2017**, *33*, 1436–1444. [[CrossRef](#)] [[PubMed](#)]
13. Schroeder, R.; Torres, F.W.; Binder, C.; Klein, A.N.; De Mello, J.D.B. Failure mode in sliding wear of PEEK based composites. *Wear* **2013**, *301*, 717–726. [[CrossRef](#)]
14. Theiler, G.; Gradt, T. Environmental effects on the sliding behaviour of PEEK composites. *Wear* **2016**, *368–369*, 278–286. [[CrossRef](#)]
15. Kvítek, O.; Fajstavr, D.; Řezníčková, A.; Kolská, Z.; Slepíčka, P.; Švorčík, V. Annealing of gold nanolayers sputtered on polyimide and polyetheretherketone. *Thin Solid Films* **2016**, *616*, 188–196. [[CrossRef](#)]

16. Ur Rehman, M.A.; Ferraris, S.; Goldmann, W.H.; Perero, S.; Bastan, F.E.; Nawaz, Q.; Confiengo, G.G.D.; Ferraris, M.; Boccaccini, A.R. Antibacterial and Bioactive Coatings Based on Radio Frequency Co-Sputtering of Silver Nanocluster-Silica Coatings on PEEK/Bioactive Glass Layers Obtained by Electrophoretic Deposition. *ACS Appl. Mater. Interfaces* **2017**, *9*, 32489–32497. [[CrossRef](#)]
17. Yameen, B.; Álvarez, M.; Azzaroni, O.; Jonas, U.; Knoll, W. Tailoring of poly(ether ether ketone) surface properties via surface-initiated atom transfer radical polymerization. *Langmuir* **2009**, *25*, 6214–6220. [[CrossRef](#)]
18. Khan, Z.; Hussain, J.I.; Kumar, S.; Hashmi, A.A. Silver nanoplates and nanowires by a simple chemical reduction method. *Colloids Surf. B Biointerfaces* **2011**, *86*, 87–92. [[CrossRef](#)]
19. Le, A.T.; Huy, P.T.; Tam, P.D.; Huy, T.Q.; Cam, P.D.; Kudrinskiy, A.A.; Krutyakov, Y.A. Green synthesis of finely-dispersed highly bactericidal silver nanoparticles via modified Tollens technique. *Curr. Appl. Phys.* **2010**, *10*, 910–916. [[CrossRef](#)]
20. Kvittek, L.; Panacek, A.; Prucek, R.; Soukupova, J.; Vanickova, M.; Kolar, M.; Zboril, R. Antibacterial activity and toxicity of silver—Nanosilver versus ionic silver. *J. Phys. Conf. Ser.* **2011**, *304*, 012029. [[CrossRef](#)]
21. Zienkiewicz-Strzałka, M.; Pasieczna-Patkowska, S.; Kozak, M.; Pikus, S. Silver nanoparticles incorporated onto ordered mesoporous silica from Tollen's reagent. *Appl. Surf. Sci.* **2013**, *266*, 337–343. [[CrossRef](#)]
22. Luo, Y.; Shen, S.; Luo, J.; Wang, X.; Sun, R. Green synthesis of silver nanoparticles in xylan solution via Tollens reaction and their detection for Hg^{2+} . *Nanoscale* **2015**, *7*, 690–700. [[CrossRef](#)] [[PubMed](#)]
23. Michalcová, A.; Machado, L.; Marek, I.; Martinec, M.; Sluková, M.; Vojtěch, D. Properties of Ag nanoparticles prepared by modified Tollens' process with the use of different saccharide types. *J. Phys. Chem. Solids* **2018**, *113*, 125–133. [[CrossRef](#)]
24. Montazer, M.; Allahyarzadeh, V. Electroless plating of silver nanoparticles/nanolayer on polyester fabric using $AgNO_3/NaOH$ and ammonia. *Ind. Eng. Chem. Res.* **2013**, *52*, 8436–8444. [[CrossRef](#)]
25. Kyriakidou, E.A.; Alexeev, O.S.; Wong, A.P.; Papadimitriou, C.; Amiridis, M.D.; Regalbuto, J.R. Synthesis of Ag nanoparticles on oxide and carbon supports from Ag diammine precursor. *J. Catal.* **2016**, *344*, 749–756. [[CrossRef](#)]
26. Le, A.T.; Tam, L.T.; Tam, P.D.; Huy, P.T.; Huy, T.Q.; Van Hieu, N.; Kudrinskiy, A.A.; Krutyakov, Y.A. Synthesis of oleic acid-stabilized silver nanoparticles and analysis of their antibacterial activity. *Mater. Sci. Eng. C* **2010**, *30*, 910–916. [[CrossRef](#)]
27. Kubiak, K.; Adamczyk, Z.; Oćwieja, M. Kinetics of Silver Nanoparticle Deposition at PAH Monolayers: Reference QCM Results. *Langmuir* **2015**, *31*, 2988–2996. [[CrossRef](#)]
28. Oćwieja, M.; Adamczyk, Z. Controlled Release of Silver Nanoparticles from Monolayers Deposited on PAH Covered Mica. *Langmuir* **2013**, *29*, 3546–3555. [[CrossRef](#)]
29. Cruz Pacheco, A.F.; Gómez Cuaspud, J.A.; Parra Vargas, C.A.; Carda Castello, J.B. Combustion synthesis, structural and magnetic characterization of $Ce_{1-x}Pr_xO_2$ system. *J. Mater. Sci. Mater. Electron.* **2017**, *28*, 16358–16365. [[CrossRef](#)]
30. Seuss, S.; Heinloth, M.; Boccaccini, A.R. Development of bioactive composite coatings based on combination of PEEK, bioactive glass and Ag nanoparticles with antibacterial properties. *Surf. Coat. Technol.* **2016**, *301*, 100–105. [[CrossRef](#)]
31. Hasegawa, S.; Sato, K.; Narita, T.; Suzuki, Y.; Takahashi, S.; Morishita, N.; Maekawa, Y. Radiation-induced graft polymerization of styrene into a poly(ether ether ketone) film for preparation of polymer electrolyte membranes. *J. Membr. Sci.* **2009**, *345*, 74–80. [[CrossRef](#)]
32. Gupta, B.; Gautam, D.; Ikram, S. Preparation of proton exchange membranes by radiation-induced grafting of alpha methyl styrene-butyl acrylate mixture onto polyetheretherketone (PEEK) films. *Polym. Bull.* **2013**, *70*, 2691–2708. [[CrossRef](#)]
33. Gümüş, S.; Polat, Ş.; Waldhauser, W.; Lackner, J.M. Biodegradation of anti-microbial titanium-magnesium-silver coatings on polyetheretherketone for bone-contact applications. *Surf. Coat. Technol.* **2017**, *320*, 503–511. [[CrossRef](#)]
34. Vaiano, V.; Matarangolo, M.; Murcia, J.J.; Rojas, H.; Navío, J.A.; Hidalgo, M.C. Enhanced photocatalytic removal of phenol from aqueous solutions using ZnO modified with Ag. *Appl. Catal. B Environ.* **2018**, *225*, 197–206. [[CrossRef](#)]

35. Chook, S.W.; Chia, C.H.; Zakaria, S.; Ayob, M.K.; Huang, N.M.; Neoh, H.M.; Jamal, R. Antibacterial hybrid cellulose-graphene oxide nanocomposite immobilized with silver nanoparticles. *RSC Adv.* **2015**, *5*, 26263–26268. [[CrossRef](#)]
36. Pal, S.; Nisi, R.; Stoppa, M.; Licciulli, A. Silver-Functionalized Bacterial Cellulose as Antibacterial Membrane for Wound-Healing Applications. *ACS Omega* **2017**, *2*, 3632–3639. [[CrossRef](#)] [[PubMed](#)]
37. El-Naggar, N.E.-A.; Hussein, M.H.; El-Sawah, A.A. Phycobiliprotein-mediated synthesis of biogenic silver nanoparticles, characterization, in vitro and in vivo assessment of anticancer activities. *Sci. Rep.* **2018**, *8*, 8925. [[CrossRef](#)]
38. Hwang, M.L.; Song, J.M.; Ko, B.S.; Sohn, J.Y.; Nho, Y.C.; Shin, J. Radiation-induced grafting of vinylbenzyl chloride onto a poly(ether ether ketone) film. *Nucl. Instrum. Methods Phys. Res. Sect. B Beam Interact. Mater. Atoms* **2012**, *281*, 45–50. [[CrossRef](#)]
39. Kim, A.R.; Vinothkannan, M.; Yoo, D.J. Sulfonated-fluorinated copolymer blending membranes containing SPEEK for use as the electrolyte in polymer electrolyte fuel cells (PEFC). *Int. J. Hydrogen Energy* **2017**, *42*, 4349–4365. [[CrossRef](#)]
40. Jean-Fulcrand, A.; Masen, M.A.; Bremner, T.; Wong, J.S.S. Effect of temperature on tribological performance of polyetheretherketone-polybenzimidazole blend. *Tribol. Int.* **2019**, *129*, 5–15. [[CrossRef](#)]
41. Girard, J.; Joset, N.; Crochet, A.; Tan, M.; Holzheu, A.; Brunetto, P.S.; Fromm, K.M. Synthesis of new polyether ether ketone derivatives with silver binding site and coordination compounds of their monomers with different silver salts. *Polymers* **2016**, *8*, 208. [[CrossRef](#)]
42. Anupama, N.; Madhumitha, G. Green synthesis and catalytic application of silver nanoparticles using Carissa carandas fruits. *Inorg. Nano-Met. Chem.* **2017**, *47*, 116–120. [[CrossRef](#)]
43. Ismail, M.; Gul, S.; Khan, M.I.; Khan, M.A.; Asiri, A.M.; Khan, S.B. Medicago polymorpha-mediated antibacterial silver nanoparticles in the reduction of methyl orange. *Green Process. Synth.* **2018**. [[CrossRef](#)]
44. Hamciuc, C.; Hamciuc, E.; Popovici, D.; Danaila, A.I.; Butnaru, M.; Rimbu, C.; Carp-Carare, C.; Kalvachev, Y. Biocompatible poly(ether-ether-ketone)/Ag-zeolite L composite films with antimicrobial properties. *Mater. Lett.* **2018**, *212*, 339–342. [[CrossRef](#)]
45. Sana, S.S.; Dogiparthi, L.K. Green synthesis of silver nanoparticles using Givotia moluccana leaf extract and evaluation of their antimicrobial activity. *Mater. Lett.* **2018**, *226*, 47–51. [[CrossRef](#)]
46. Yu, D.; Yam, V.W.W. Hydrothermal-induced assembly of colloidal silver spheres into various nanoparticles on the basis of HTAB-modified silver mirror reaction. *J. Phys. Chem. B* **2005**, *109*, 5497–5503. [[CrossRef](#)] [[PubMed](#)]
47. Sharma, V.K.; Yngard, R.A.; Lin, Y. Silver nanoparticles: Green synthesis and their antimicrobial activities. *Adv. Colloid Interface Sci.* **2009**, *145*, 83–96. [[CrossRef](#)] [[PubMed](#)]
48. Kvítek, L.; Pucek, R.; Panáček, A.; Novotný, R.; Hrbáč, J.; Zbořil, R. The influence of complexing agent concentration on particle size in the process of SERS active silver colloid synthesis. *J. Mater. Chem.* **2005**, *15*, 1099–1105. [[CrossRef](#)]
49. Panáček, A.; Kvítek, L.; Pucek, R.; Kolář, M.; Večeřová, R.; Pizúrová, N.; Sharma, V.K.; Nevěčná, T.; Zbořil, R. Silver Colloid Nanoparticles: Synthesis, Characterization, and Their Antibacterial Activity. *J. Phys. Chem. B* **2006**, *110*, 16248–16253. [[CrossRef](#)]
50. Sun, M.; Feng, J.; Bu, Y.; Luo, C. Nanostructured-silver-coated polyetheretherketone tube for online in-tube solid-phase microextraction coupled with high-performance liquid chromatography. *J. Sep. Sci.* **2015**, *38*, 3119–3304. [[CrossRef](#)]
51. Corni, I.; Neumann, N.; König, K.; Veronesi, P.; Chen, Q.; Ryan, M.P.; Boccaccini, A.R. Electrophoretic deposition of PEEK-nano alumina composite coatings on stainless steel. *Surf. Coat. Technol.* **2009**, *203*, 1349–1359. [[CrossRef](#)]
52. Rolim, W.R.; Pelegrino, M.T.; de Araújo Lima, B.; Ferraz, L.S.; Costa, F.N.; Bernardes, J.S.; Rodrigues, T.; Brocchi, M.; Seabra, A.B. Green tea extract mediated biogenic synthesis of silver nanoparticles: Characterization, cytotoxicity evaluation and antibacterial activity. *Appl. Surf. Sci.* **2019**, *463*, 66–74. [[CrossRef](#)]
53. El-Faham, A.; Atta, A.M.; Osman, S.M.; Ezzat, A.O.; El-saeed, A.M.; AL Othman, Z.A.; Al-Lohedan, H.A. Silver-embedded epoxy nanocomposites as organic coatings for steel. *Prog. Org. Coat.* **2018**, *123*, 209–222. [[CrossRef](#)]

54. Chen, J.; Li, D.; Koshikawa, H.; Zhai, M.; Asano, M.; Oku, H.; Maekawa, Y. Modification of ultrathin polyetheretherketone film for application in direct methanol fuel cells. *J. Membr. Sci.* **2009**, *344*, 266–274. [[CrossRef](#)]
55. Liu, X.; Gan, K.; Liu, H.; Song, X.; Chen, T.; Liu, C. Antibacterial properties of nano-silver coated PEEK prepared through magnetron sputtering. *Dent. Mater.* **2017**, *33*, 348–360. [[CrossRef](#)] [[PubMed](#)]
56. Felix, T.; Cassini, F.A.; Benetoli, L.O.B.; Dotto, M.E.R.; Debacher, N.A. Morphological study of polymer surfaces exposed to non-thermal plasma based on contact angle and the use of scaling laws. *Appl. Surf. Sci.* **2017**, *403*, 57–61. [[CrossRef](#)]
57. Li, W.; Chen, Y.; Wu, S.; Zhang, J.; Wang, H.; Zeng, D.; Xie, C. Preparing high-adhesion silver coating on APTMS modified polyethylene with excellent anti-bacterial performance. *Appl. Surf. Sci.* **2018**, *436*, 117–124. [[CrossRef](#)]
58. Cervantes-García, E.; García-González, R.; Salazar-Schettino, P.M. Proteínas de membrana externa de *Serratia marcescens*. *Revista Latinoamericana de Patología Clínica y Medicina de Laboratorio* **2014**, *61*, 224–228.
59. Baghayeri, M.; Mahdavi, B.; Hosseinpour-Mohsen Abadi, Z.; Farhadi, S. Green synthesis of silver nanoparticles using water extract of *Salvia leriifolia*: Antibacterial studies and applications as catalysts in the electrochemical detection of nitrite. *Appl. Organomet. Chem.* **2017**, *32*, e4057. [[CrossRef](#)]
60. Thaya, R.; Malaikozhundan, B.; Vijayakumar, S.; Sivakamavalli, J.; Jeyasekar, R.; Shanthi, S.; Vaseeharan, B.; Ramasamy, P.; Sonawane, A. Chitosan coated Ag/ZnO nanocomposite and their antibiofilm, antifungal and cytotoxic effects on murine macrophages. *Microb. Pathog.* **2016**, *100*, 124–132. [[CrossRef](#)]
61. Umoren, S.A.; Nzila, A.M.; Sankaran, S.; Solomon, M.M.; Umoren, P.S. Green synthesis, characterization and antibacterial activities of silver nanoparticles from strawberry fruit extract. *Pol. J. Chem. Technol.* **2017**, *19*, 128–136. [[CrossRef](#)]
62. Sikder, P.; Grice, C.R.; Lin, B.; Goel, V.K.; Bhaduri, S.B. Single-Phase, Antibacterial Trimagnesium Phosphate Hydrate Coatings on Polyetheretherketone (PEEK) Implants by Rapid Microwave Irradiation Technique. *ACS Biomater. Sci. Eng.* **2018**, *4*, 2767–2783. [[CrossRef](#)]
63. Sikder, P.; Koju, N.; Ren, Y.; Goel, V.K.; Phares, T.; Lin, B.; Bhaduri, S.B. Development of single-phase silver-doped antibacterial CDHA coatings on Ti6Al4V with sustained release. *Surf. Coat. Technol.* **2018**, *342*, 105–116. [[CrossRef](#)]
64. Mosselhy, D.; Granbohm, H.; Hynönen, U.; Ge, Y.; Palva, A.; Nordström, K.; Hannula, S.-P. Nanosilver–Silica Composite: Prolonged Antibacterial Effects and Bacterial Interaction Mechanisms for Wound Dressings. *Nanomaterials* **2017**, *7*, 261. [[CrossRef](#)] [[PubMed](#)]
65. Yue, X.; Zhang, T.; Yang, D.; Qiu, F.; Li, Z.; Wei, G.; Qiao, Y. Ag nanoparticles coated cellulose membrane with high infrared reflection, breathability and antibacterial property for human thermal insulation. *J. Colloid Interface Sci.* **2018**, *535*, 363–370. [[CrossRef](#)] [[PubMed](#)]
66. Logeswari, P.; Silambarasan, S.; Abraham, J. Synthesis of silver nanoparticles using plants extract and analysis of their antimicrobial property. *J. Saudi Chem. Soc.* **2015**, *19*, 311–317. [[CrossRef](#)]
67. Gao, L.; Gan, W.; Xiao, S.; Zhan, X.; Li, J. A robust superhydrophobic antibacterial Ag-TiO₂ composite film immobilized on wood substrate for photodegradation of phenol under visible-light illumination. *Ceram. Int.* **2016**, *42*, 2170–2179. [[CrossRef](#)]

